Solvent Effect on Intramolecular Electron Transfer Rates of Mixed-Valence Biferrocene Monocation Derivatives

Y. Masuda* and C. Shimizu

Department of Chemistry, Faculty of Science, Ochanomizu University, Bunkyo-ku, Tokyo 112-8610

Received: January 5, 2006; In Final Form: April 6, 2006

Intramolecular electron transfer (ET) rates in various solvents of mixed-valence biferrocene monocation (Fe(II), Fe(III)) and the 1′,1‴-diiodo and 1′,1‴-diethyl derivatives (respectively abbreviated as BFC^+, I_2BFC^+, and Et_2BFC^+) were determined by means of the spin−lattice relaxation times of the protons, taking into account the local magnetic field fluctuation caused by the electron hopping between the two ferrocene units. We also determined the ET rates of a mixed-valence diferrocenylacetylene monocation (DFA^+) in order to examine the effect of the insertion of an acetylene bridge between the two ferrocene units. The insertion of the bridge decreased the ET rate, while the effect of substitution on the cyclopentadienyl rings on the rate was minor. The observed rates for each mixed-valence monocation in various solvents did not correlate with the reorganization energies, but we did find a significant contribution of the solvent dynamics. The observed rates were considerably higher than those expected on the basis of the Sumi−Marcus−Nalder model in which the solvents were regarded as dielectric continua. The slope of the logarithm plot of the pre-exponential factors in various solvents for each mixed-valence monocation versus the inverse of the longitudinal dielectric relaxation times of the solvents was significantly smaller than unity, and the slope for DFA^+ was larger than those for BFC^+, I_2BFC^+, and Et_2BFC^+. These results were ascribed to a partial contribution of the dielectric friction to the dynamics along the solvent coordinate; the extent of the contribution decreased with a reduction in the ET distance. For the dynamics along the solvent coordinate of the ET reactions in methanol, the observed rates indicated an important contribution by the minor dielectric relaxation components with faster relaxation times, rather than the major component with an extraordinarily long relaxation time.

1. Introduction

In electron transfer (ET) rates in solutions, the solvent often plays an important role because of the strong electrostatic coupling between the migrating charge and the solvent.[1] The solvent effect on the rates has usually been dealt with by a model, devised by Marcus in the 1950s, that considered the static contribution of the solvent;[2,3] i.e., the solvent-dependent rate is ascribed to a solvation-induced change in the free energies of the reactant and the product. On the other hand, remarkable progress in the experimental and theoretical studies of ultrafast charge transfer processes within the last two decades has provided new points of view to understand the solvent effect on ET reactions. One of the most important outcomes of these studies is the confirmation of the contribution of the dynamic properties of the solvent to the reaction rates.[1,4−9]

Various models of such a "dynamical solvent effect" currently exist. One of the most representative treatments is presented by Sumi, Marcus, and Nadler in their two-dimensional model.[10,11] They divided a reaction into two processes based on a difference in the time scale: The first is a reaction along a coordinate expressing the nuclear position changes brought about by internal vibrations (the internal coordinate); the second is marked by a solvation free energy change with a fluctuation of the surrounding solvent (the solvent coordinate). In the model, the contribution of solvent dynamics to the rate is treated as a friction for the dynamics along the solvent coordinate.

In the dynamics along the solvent coordinate, the solvent is often regarded as a dielectric continuum. On the other hand, a contribution of the inertial or local modes of the solvent with a faster time scale than the dielectric relaxation is found in red shifts in time-resolved fluorescence spectra, which directly reflect the solvation process occurring after a change in the charge distribution of a solute,[4,12] as well as in computer simulation results.[12,13] The contribution of such fast solvent modes is, in fact, taken into consideration for the interpretation of rates in some ET systems.[14] Moreover, molecular dynamics (MD) simulations and theoretical predictions indicate that the (average) relaxation time of the solvation free energy depends on the size of the probe molecule and on the magnitude of the instantaneous change in the dipole moment.[13] These experimental results and theoretical predictions suggest that the extent of the contribution of the dielectric relaxation mode to the dynamics along the solvent coordinate of an ET reaction depends on the magnitude of the displacement of the spatial charge distribution accompanying the ET reaction. The verification from this point of view by systematic experimental studies would be an indispensable benchmark for the refinement of models or theories involving a coupling between a reaction system and its environmental dynamics.

For this purpose, we have focused on the intramolecular ET reactions of the biferrocene monocation (Fe(II), Fe(III)), BFC^+, and its derivatives, which are assigned to the class-II-type mixed-valence monocations.[15] In our previous papers, we reported intramolecular ET rates of BFC^+ on the picosecond time scale, which were obtained by the detection of the nuclear spin

* E-mail: masuda@cc.ocha.ac.jp.

10.1021/jp060087w CCC: $33.50
Published on Web 05/17/2006

SCHEME 1

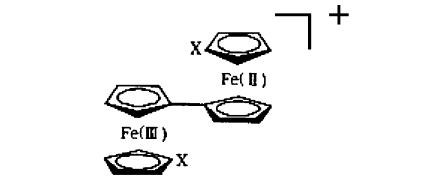

X = H : biferrocene monocation (BFC^+)
X = Et : 1,1‴-diethylbiferrocene monocation (Et_2BFC^+)
X = I : 1,1‴-diiodebiferrocene monocation (I_2BFC^+)

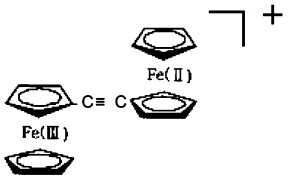

diferrocenylacetylene monocation (DFA^+)

relaxation caused by a local magnetic field fluctuation accompanying the electron hopping between the two ferrocene units.[16] In the present paper, we compare the solvent dependence of the ET rate of BFC^+ with the analogous mixed-valence monocations with ethyl or iodine substituents on the cyclopentadienyl rings and with an acetylene bridge between the two ferrocene units (Scheme 1). The substitution produces a change in the molecular volume, and the insertion of the bridge brings about a change in the ET distance. A comparison of the solvent dependences of the observed ET rates of these mixed-valence monocations is, therefore, expected to demonstrate how a variation in the magnitude of the electric field change accompanying the ETs is related to the extent of the contribution of the solvent dielectric relaxation mode to the ET rates.

The present intramolecular ET system has no driving force (i.e., it has a symmetrical ET potential), and both the reactant and the product are in the electronic ground states, so that the system is thermally equilibrated. In contrast, most of the previously studied ultrafast ET reaction systems contain photoexcited state(s) because of the use of a pulse laser technique. Such ET processes, after photoexcitations, usually have large driving forces.[1] In this situation, the participation of the highly vibrational excited states of the product in the ET reaction sometimes make a significant contribution to the observed rate, since the vibrational states enable a multichannel transition between the reactant and the product.[14,17,18]

The reaction system of the present mixed-valence biferrocenes is free from such complications of the reaction path that sometimes cause difficulties in the extraction of the dynamical contribution of thesolvent to the rates. Additionally, the ET reactions in these systems are rather general, and still fundamental in the fields of chemistry and biology, and commonly occur in many inorganic[19] and organic[20] mixed-valence systems. Nevertheless, quantitative information on the intramolecular ET rate constants exceeding 10^{11} s^{-1} has been reported only for the biferrocene monocation (BFC^+) and for the mixed-valence dimers of trinuclear ruthenium triacetates.[21]

2. Experimental Section

2.1. Materials. Biferrocene (BFC), 1′,1‴-diiodobiferrocene (I_2BFC), 1′,1‴-diethylbiferrocene (Et_2BFC), and diferrocenylacetylene (DFA) were synthesized by literature methods.[22−26] The hexafluorophosphate salts of the mixed-valence biferrocene monocations of BFC, I_2BFC, and Et_2BFC were prepared by modifying a method previously reported.[16a] A methanol solution of 0.1 M HPF_6 was added dropwise to a benzene or dichloromethane solution containing a biferrocene or a derivative and a small excess of *p*-benzoquinone cooled with ice, and was stirred for 20−30 min. The precipitates of the mixed-valence monocations were collected and recrystallized from dichloromethane or benzene. When the same procedure was applied to obtain the hexafluorophosphate salt of DFA^+, the dication salt, $DFA(PF_6)_2$, was precipitated. The solutions of DFA^+ for the spectroscopic measurements were prepared by dissolving the equimolar mixture of the dication salt, $DFA(PF_6)_2$, and the neutral DFA. All the above procedures were carried out under a dry argon atmosphere.

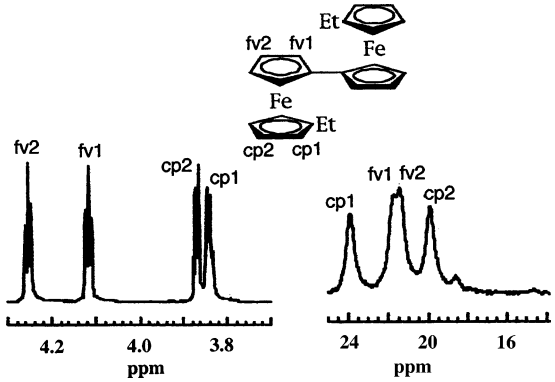

Figure 1. NMR spectra of 1′,1‴-diethylbiferrocene (left) and the mixed-valence monocation (right) at 298 K in acetone.

2.2. Spectroscopic Measurements. The ^1H NMR spectra were obtained with a JEOL GSX-400 or an AL-400 Fourier transform spectrometer operating at 400 MHz. The spin−lattice relaxation times, T_1, were measured by an inversion−recovery method. The chemical shifts were determined by the use of trimethylsilane (TMS) as an internal reference. The measurements were performed with 5-mm (o.d.) cylindrical tubes, and the temperature was controlled within ±0.5 °C. The X-band electron spin resonance (ESR) spectra were measured with a JEOL FE-ESR spectrometer at a 9.1 GHz microwave frequency. The near-IR spectra were measured with a Shimazu UV 3100PC spectrophotometer. The band maxima and the widths for the intervalence transitions were determined by Gaussian curve fitting.

The sample solutions for the spectral measurements were prepared by distilling the solvents into sample tubes with the mixed-valence monocation salts under vacuum, and the tubes were torch-sealed. These procedures were carried out with a vacuum line. The solvents had previously been dried and degassed. The deuterated solvents (>99.9 atom %, provided by Isotec, Inc., or Aldrich, Inc.) were used for the NMR measurements without further purification. The protiated solvents for the other measurements were dried and distilled by the usual methods before use.

The NMR and ESR measurements for the biferrocene monocation salt solutions were carried out at concentrations of about 0.5 mM of the salts unless otherwise noted.

In the NMR spectra of the fulvalene and the cyclopentadienyl moieties, the protons of the monocation of the mixed-valence biferrocene derivatives partially overlapped, as shown in Figure 1. Each intensity and position of each peak needed to obtain the proton T_1value and the shift were determined by a Lorentzian curve fitting method.

2.3. ^1H NMR Signal Assignment of the Mixed-Valence Monocations. The ^1H signal assignment for the mixed-valence monocations was carried out by the following procedure. Small amounts of an acetone solution of iodine were successively

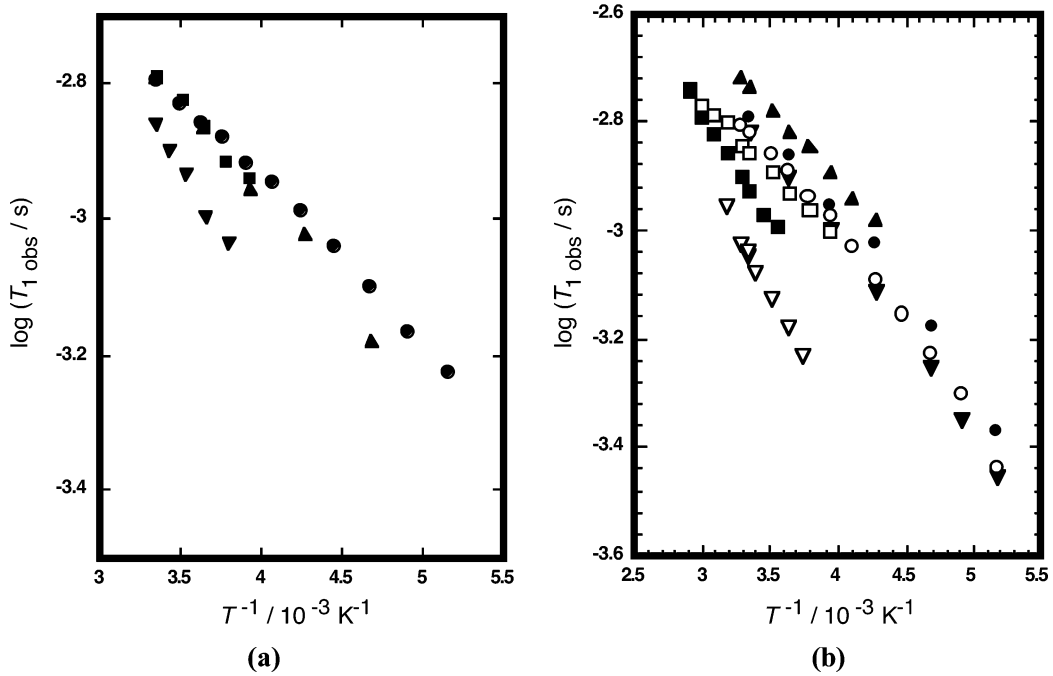

Figure 2. Averaged values of the observed T_1 of protons of bridging groups in mixed-valence biferrocene monocations. (a) BFC^+(closed circle), Et_2BFC^+ (closed triangle), I_2BFC^+ (closed square), and DFA^+ (closed inverted triangle) in acetone. (b) The T_1 values for Et_2BFC^+ in acetone (closed circle), acetonitrile (closed triangle), dichloromehane (open circle), nitromethane (open square), nitrobenzene (closed square), methanol (closed inverted triangle), and ethylene glycol (open inverted triangle).

added to an acetone solution of each neutral biferrocene. The correspondences of the respective proton signals of each mixed-valence monocation to those of the neutral were determined by plotting the observed shifts against the fraction of the mixed-valence monocation oxidized by the added iodine. The signal assignments for the neutral monocations were determined on the basis of the results of the H−H correlation spectroscopy (COSY) and the proton T_1 measurements.[27]

3. Results

3.1. Determination of the Intramolecular ET Rate Constants. The electron hopping (intramolecular ET) between the two iron atoms causes a fluctuation of the local magnetic field at the protons in the mixed-valence monocation. The intramolecular ET rates were determined from the observation of the proton spin−lattice relaxation caused by the fluctuation. The procedure in detail is given in our previous paper.[16a]

The spin−lattice relaxation times of the fulvalene protons of the mixed-valence monocations were used for the determination of the ET rates, since the internal rotations of the cyclopentadienyl rings around the pseudo C_5 axes contributed to the cyclopentadienyl proton relaxations.[28] The inverse of the observed spin−lattice relaxation times for the two kinds of fulvalene protons, labeled fv1 and fv2 in Figure 1, were averaged, because the difference in the values was within the experimental error. The averaged values, $T_{1,obs}$, are shown in Figure 2 and in the Supporting Information.[29] Considering the rapid electron hopping between the two iron atoms and the much shorter $T_{1,obs}$ values than those for the respective neutral monocations, e.g., the values are 13 s and 1.6 ms, respectively, for I_2BFC and I_2BFC^+ in acetone at 298 K, the proton relaxation rate due to the interaction with the unpaired electron, $T_{1\,para}^{-1}$, is then denoted by[30]

$$T_{1\,para}^{-1} \approx 2T_{1\,obs}^{-1} \tag{1}$$

The relaxation rate thus obtained, T_{1para}^{-1}, mainly consists of two terms: the first, denoted as T_{1dip}^{-1}, is due to the magnetic dipolar interaction, and the second, labeled T_{1hyp}^{-1}, is due to the hyperfine interaction with the electron spin. Thus

$$T_{1para}^{-1} = T_{1dip}^{-1} + T_{1hyp}^{-1} \tag{2}$$

The respective terms in eq 2 in common liquids are represented by[31,32]

$$T_{1dip}^{-1} = K_{dip}\,[3\tau_{c1} + 7\tau_{c2}/(1 + \omega_S^2\tau_{c2}^2)\,] \tag{3a}$$

$$K_{dip} = (2/10)\gamma_H^2 g^2 \beta^2 r_{IS}^{-6} \tag{3b}$$

$$T_{1hyp}^{-1} = K_{hyp}\,[\tau'_{c2}/(1 + \omega_S^2\tau'^2_{c2})] \tag{4a}$$

$$K_{hyp} = (1/2)(A/\hbar)^2 \tag{4b}$$

In these equations, ω_S, γ_H, β, A, and r_{IS} represent, respectively, the Larmor frequency of the electron spin, the gyromagnetic ratio of the observed nucleus, the Bohr magneton, the hyperfine parameter, and the distance between the nucleus and the electron spin. The value of g^2 is given by the relation, $g^2 = (g_\parallel^2 + 2g_\perp^2) + g_\parallel^2 \cos^2\theta + g_\perp^2 \sin^2\theta$, where $g_\parallel$ and $g_\perp$ indicate the parallel and perpendicular g values, respectively, and θ is the angle between the main axis of the g tensor and the vector connecting an observing proton and the electron spin.

The variables, τ_{c1}, τ_{c2}, and τ'_{c2}, in eqs 3a and 4a are the correlation times of the fluctuations of the magnetic interaction (see below). These fluctuations are caused not only by the reorientational motion of the monocation and the electron spin relaxation, but also by the electron hopping (the electron transfer) between the two iron atoms. For example, the change in the distance between an observing proton and the unpaired electron spin in the mixed-valence monocation, r_{IS}, due to the ET generates a significant fluctuation of the local magnetic field at the proton, because the field depends on r_{IS}^{-6}, as shown in eq 3b.[31−33] The correlation times are then represented by[16]

$$\tau_{c1}^{-1} = \tau_r^{-1} + T_{1e}^{-1} + k_{et} \quad (5a)$$

$$\tau_{c2}^{-1} = \tau_r^{-1} + T_{2e}^{-1} + k_{et} \quad (5b)$$

$$\tau_{c'2}^{-1} = T_{2e}^{-1} + k_{et} \quad (5c)$$

where τ_r, T_{1e}, T_{2e}, and k_{et} denote the reorientational correlation time of the monocation, the spin−lattice and the spin−spin electron spin relaxation time, and the ET rate constant, respectively. If the ET rate is comparable to, or even faster than, the molecular reorientation and the electron spin relaxation, k_{et} significantly contributes to τ_c^{-1}.

In the case of BFC^+, τ_r and T_{2e} ($\leq T_{1e}$) are, respectively, estimated to be 8×10^{-11} s and $\gg 7 \times 10^{-11}$ s in acetone at 298 K.[16] These values are significantly larger than the observed value of $\tau_{1c} \approx \tau_{2c} \approx \tau'_{2c} \approx 2.9 \times 10^{-12}$ s, that is, these correlation times are approximately equal to k_{et}^{-1}.[34] The rotational correlation times of Et_2BFC^+, I_2BFC^+, and DFA^+ are expected to be longer than that for the biferrocene monocation, because the molecular volumes of these derivatives are larger than that of BFC^+.[35] The electron spin−spin relaxation times, $T_{2e} \leq T_{1e}$, of the mixed-valence biferrocene derivatives are estimated to be similar to or longer than those for BFC^+.[36,37] Consequently, the approximation, $\tau_{1c} \approx \tau_{2c} \approx \tau'_{2c} \approx k_{et}^{-1}$, is also valid for the present mixed-valence biferrocene derivatives.

The intramolecular ET rate can thus be determined from the observed relaxation time, T_{1obs}, if one obtains the values of K_{dip} and K_{hyp} in eqs 3 and 4, respectively. The K_{dip} value for each mixed-valence monocation is given by the $g_{||}$ and $g_\perp$ values and the geometry of the mixed-valence monocation. The $g_{||}$ and $g_\perp$ values were given by ESR measurements in frozen solutions and are listed in Table 2.[38,39] The r_{IS} and θ values were obtained on the basis of the X-ray crystal data.[15d,39−41] The K_{hyp} values are given by the hyperfine parameters, $(A/\hbar)$, which themselves were determined from the proton paramagnetic shifts;[31,32] the results are shown in Table 1. (The detailed procedure to determine the values is provided in the Appendix.) The K_{1hyp} values thus estimated were much smaller than the K_{dip} values for the corresponding mixed-valence monocations, which implies that

$$2T_{1obs}^{-1} \approx T_{1para}^{-1} \approx T_{1dip}^{-1}$$

The intramolecular ET rates, k_{et}, thus determined from the observed T_{1obs} values in various solvents and at various temperatures, are given in the Supporting Information.

3.2. Reorganization Energies and Electronic Coupling Elements. The observed band maxima of the intervalence transitions (ITs) of the mixed-valence biferrocene derivatives, E_{op}, are linked to the reorganization energies, λ, by the following relation:[42]

$$E_{op} = \lambda = \lambda_{is} + \lambda_{os} \quad (6)$$

Here, λ_{is} and λ_{os} represent the internal and outer sphere reorganization energies, respectively.

The electronic couplingvalue, H_{ab}, for each mixed-valence monocation was estimated from the IT band spectra and the change in the dipole moment for the intervalence transition according to Hush relation.[42−44] The values of H_{ab} in acetone are listed in Table 2. The effect of the band shift and the change in the intensity in different solvents on the H_{ab} values was comparable to or even smaller than the inaccuracy in the measurements. Thus, the H_{ab} value for each mixed-valence monocation in acetone was commonly used in the other solvents. The electronic couplings thus obtained were significantly decreased by the insertion of an acetylene bridge between the two ferrocene units; however, the effect of the substitution on the cyclopentadienyl rings was minor. Such a trend in the magnitude of the mixing of the electronic states of the reactant and the product is also suggested by the first and second redox potential difference, $\Delta E_{1,2}$,[45] due to a stabilization of the mixed-valence states, as shown in Table 2.

The internal reorganization energy for BFC^+ is estimated to be 33 kJ mol^{-1} by Williams et al.,[46] who take into account the three internal vibrational modes: the cp-Fe-cp stretching mode (294 cm^{-1}), the cp-Fe-cp bending mode (504 cm^{-1}), and the ring breathing mode (1100 cm^{-1}). They also considered the respective normal coordinate displacements of the reactant/product, which were given by the time-dependent analyses of the resonance Raman scattering intensities. On the other hand, if the solvents are regarded as a dielectric continuum, the internal reorganization energy for each mixed-valence monocation could be estimated from the intercepts of the plot of the total reorganization energies, λ, versus the Pekar factors of the solvents, $\epsilon_{op}^{-1} - \epsilon_S^{-1}$, where ϵ_{op} and ϵ_S are the optical and static dielectric constants, respectively.[48] Plots of λ versus $\epsilon_{op}^{-1} -$

TABLE 1: Proton NMR Shifts and *g* Values of Mixed-Valence Biferrocene Monocations

	$g_{||}$	$g_\perp$	$(\Delta\nu/\nu_0)_{obs}$[h,i] ppm	$(\Delta\nu/\nu_0)$dip[h] ppm	$(\Delta\nu/\nu_0)$hyp[h] ppm	A/h[h] 10^6 s^{-1}
Fc^+	4.35[a]	1.26[a]				
BFC^+	3.40[b]	1.63[b]	−19.5 (−4.26)	5.1	−35.6	7.9
	3.38[c]	1.67[c]				
	3.35[d]	1.60[d]				
	3.20[e]	1.52[e]				
Et_2BFC^+	2.92[e]	1.92[e]	−30.3 (−4.19)	3.8	−34.1	7.2
	3.18[f]	1.81[f]				
I_2BFC^+	3.34[e]	1.78[e]	−20.5 (−4.29)	3.7	−36.1	7.6
	3.15[f]	1.84[f]				
	3.05[g]	1.89[g]				
DFA^+	3.33[f]	1.80[f]	−17.1 (−4.30)	0.6	−26.1	5.4

[a] Measured in the frozen acetone solution of the PF_6^- salt at 20 K (ref 37). [b] Measured in the frozen acetone solution of the BF_4^- salt at 98 K (ref 16a). [c] Measured in the frozen acetone solution of the BF_4^- salt at 170 K (ref 16a). [d] Measured in the frozen methanol solution of the BF_4^- salt at 170 K (ref 16a). [e] Measured for the powder sample of the PF_6^- salt at 98 K. [f] Measured in the frozen acetone solution of the PF_6^- salt at 98 K. [g] Measured in the frozen acetonitrile solution of the PF_6^- salt at 98 K. [h] The average values of the shifts from TMS for the two fulvalene protons in acetone-d_6 at 298 K. [i] The values in parentheses indicate shifts for the neutral complexes.

TABLE 2: Electron Transfer Rate Constants, Reorganization Energies, and Electrochemical Data of Biferrocene Monocations at 298 K in Acetone

	BFC^+	Et_2BFC^+	I_2BFC^+	DFA^+
k_{et} (10^{11} s^{-1})	3.5	3.4	3.5	1.0
E_{op} (cm^{-1})	5640	5400	5490	7510
ϵ (cm^{-1} mol L^{-1})	750	812	730	425
λ_{is} (kJ/mol)	37	37	37	52
λ_{os} (kJ/mol)	31	28	29	37
H_{ab} (kJ/mol)	10.8	12.1	10.4	8.1
$E_{1/2}$ (+1/0)	0.36[a]	0.28[a]	0.49[b]	0.46[c]
$E_{1/2}$ (+2/+1)	0.68[a]	0.63[a]	0.81[b]	0.60[c]
$\Delta E_{1/2}$	0.32[a]	0.35[a]	0.32[b]	0.14[c]

[a] The measurements are run in 0.1 M *n*-Bu_4NClO_4 acetonitrile solution (ref 45a). [b] The measurements are run in 0.1 M *n*-Bu_4NClO_4 acetonitrile solution (ref 45b). [c] The measurements are run in 0.1 M *n*-Bu_4NPF_6 dichloromethane solution (ref 45c).

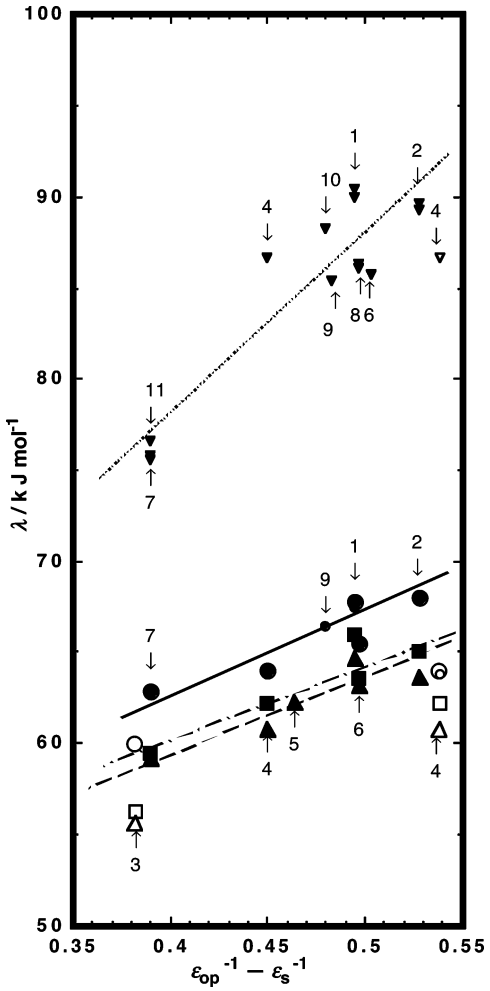

Figure 3. Plots of reorganization energies, λ, for mixed-valence biferrocene monocations in various solvents against the Pekar factors ($\epsilon_{op}^{-1} - \epsilon_s^{-1}$), where ϵ_{op} and ϵ_s are the respective solvent optical and static dielectric constants: BFC^+ (closed circle), Et_2BFC^+ (closed triangle), I_2BFC^+ (closed square), and DFA^+ (closed inverted triangle), except for those in dichloromethane and methanol, which are indicated by open symbols. The closed symbols for methanol are plots against the Pekar factor corresponding to the fastest relaxation assuming multiple (three) dielectric relaxations of the solvent, $\epsilon_{op}^{-1} - \epsilon_3^{-1}$. The large and small symbols, respectively, indicate the data from the present study and from literature reports (refs 45c and 48). The numbers in the figure indicate the following: 1, acetone; 2, acetonitrile; 3, dichloromethane; 4, methanol; 5, ethylene glycol; 6, nitromethane; 7, nitrobenzene; 8, propyronitrile; 9, butyronitrile; 10, benzonitrile; 11, propylene carbonate. Solid, dashed, dot−dashed, and dotted lines indicate the least-squares fitting results, respectively, for BFC^+, Et_2BFC^+, I_2BFC^+, and DFA^+. For the fitting, the data in dichloromethane are excluded. For methanol, the plots against the Pekar factor corresponding to the fastest relaxation assuming multiple (three) dielectric relaxations of the solvent, $\epsilon_{op}^{-1} - \epsilon_3^{-1}$, are used for the fitting insted of those against $\epsilon_{op}^{-1} - \epsilon_s^{-1}$.

ϵ_S^{-1} for the present mixed-valence monocations are shown in Figure 3. Though the plots for BFC^+, Et_2BFC^+, and I_2BFC^+ contained considerable scatter, they exhibit comparable slopes and 0-intercepts: The 0-intercepts were, respectively, ~36, ~37, and ~40 kJ mol^{-1} for BFC^+, Et_2BFC^+, and I_2BFC^+.[49] (The appreciable deviations in dichloromethane and in alcohols marked by open symbols will be discussed in sections 4.2 and 4.3.) Here, the inner-sphere reorganization energies of Et_2BFC^+ and I_2BFC^+ are assumed to be an average value of the observed 0-intercepts, 37 kJ mol^{-1}, for the following reasons: (i) Similar intercepts were found in the Pekar plots. (ii) These intercept values are close to the λ_{is} value of BFC^+, 33 kJ mol^{-1}, determined on the basis of the resonance Raman measurements.[46,47] (iii) Some properties of these mixed-valence monocations are similar to each other, e.g., the metal−ligand distances,[50] the separations in the first and the second redox potential, ΔE_{12},[45] the electronic coupling elements, and the hyperfine parameters of the fulvalene protons. (See Table 2.)

The Pekar plots for DFA^+ were generally linear except those in dichloromethane and methanol, which are represented by open symbols as shown in Figure 3. The 0-intercept in the plot has a value of 52 kJ mol^{-1}, significantly higher than the λ_{is} value for BFC^+ (37 kJ mol^{-1}). The internal reorganization energy of DFA^+ is expected to be higher than those of R_2BFC^+ (R = H, Et, and I) for the following reasons: the higher frequency shift of the IT band, the smaller electronic coupling element, the longer ET distance, and the larger separation in the first and second redox potentials.[45] Considering these facts, the use of the value of 52 kJ mol^{-1} for λ is of DFA^+ is practically acceptable.

The outer sphere reorganization energies are given by the electronic coupling elements and the internal reorganization energies estimated above. As shown in Table 2, the λ_{os} values thus obtained were increased by the insertion of an acetylene bridge.

4. Discussion

4.1. ET Rates. The observed intramolecular ET rate constants for the present mixed-valence biferrocenes, k_{et}, ranged between $1-4 \times 10^{11}$ s^{-1} at room temperature. The present rate data represent a unique report of thermally equilibrated intramolecular ET rates, except for those of the mixed-valence dimers of trinuclear ruthenium clusters bridged by pyrazine or bipyridine.[21] The ET rates of the ruthenium complexes are similar to, or even faster than, those for the mixed-valence biferrocenes, despite the twofold or higher reorganization energies of the former. These excessively high rates for the ruthenium complexes may have originated in their much larger electronic coupling elements, $H_{ab} \approx 24$ kJ mol^{-1}.

The ET rates obtainedfor DFA^+ might be compared with those for "*hypothetical* intramolecular ET rates" in the precursor complex of Fc^+ and Fc^0 in the course of their self-exchange reaction**,** because the ET distance in the precursor complex of the Fc^+/Fc^0 is assumed to be similar to that in DFA^+.[51,52] The observed rates for DFA^+ in the present study are nearly 2 orders of magnitude higher, the difference that could be attributed to the importance of the bond-through interaction between the two iron atoms in the ET. However, we do not dwell on this point, because the estimation of the hypothetical intramolecular ET rates in the precursor complex from the observed self-exchange rates contains ambiguities, and because the information about the reaction parameters of the precursor complex is poor.

The insertion of an acetylene bridge between the ferrocene and the ferrocenium unit clearly engendered a decrease in the ET rates and an increase in the temperature slopes, as shown in Table 2 and Figure 4**.** These changes correspond to an increase in the reorganization energy. On the other hand, the substitution on the cp rings by iodine or ethyl groups had a minor effect.

4.2. Dynamical Solvent Effect on k_{et}. The solvent dependence in the observed rates of each monocation did not correlate with the reorganization energies (see Figure 3). On the other hand, as depicted in Figure 5, noticeable decreases in the rates were observed in highly viscous solvents such as dinitrobenzene and ethylene glycol, despite the fact that their reorganization energies were comparable to, or even lower than, those of the

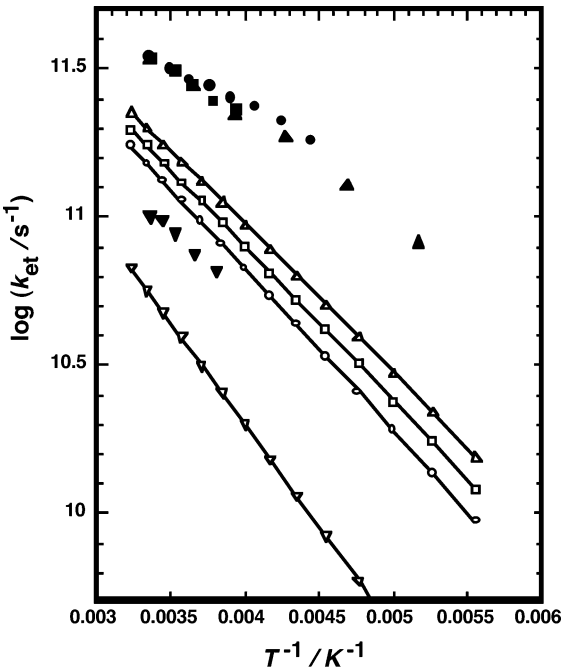

Figure 4. Temperature dependences of the observed rate constants for BFC^+ (closed circle), Et_2BFC^+ (closed triangle), I_2BFC^+ (closed square), and DFA^+ (closed inverted triangle) in acetone. The open small symbols indicate the rates calculated with eq 7, assuming $\tau_s = \tau_L$.

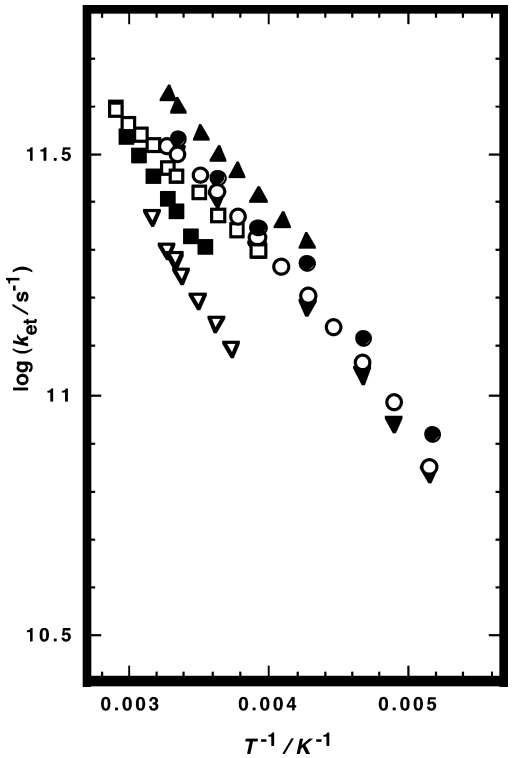

Figure 5. The observed ET rate constants for Et_2BFC^+ in acetone (closed circle), acetonitrile (closed triangle), dichloromethane (open circle), nitromethane (open square), nitrobenzene (closed square), methanol (closed inverted triangle), and ethylene glycol (open inverted triangle) at 298 K.

other solvents. This result suggested a contribution of the dynamic properties of the solvent to the rates.

The solvent effect on the rates was treated by separating the reaction into two processes on the basis of the Sumi−Marcus−Nadler model:[10,11] (i) The system diffuses, suffering solvent friction along the solvent polarization axis, x; and (ii) at a certain position on the solvent coordinate, the system reacts along the internal vibrational coordinate, q, with a rate, $k_i(x)$. For reversible ET systems, the formulation and numerical calculations for ET rates under various conditions are given by Zhu et al.[53]

In the present system, the barrier for the reaction along the internal coordinate, $\lambda_{is}/4$, is of a similar order to the zero point energies of the internal vibrations involved in the reaction, e.g., about 300 cm^{-1} for the cp-Fe-cp stretching mode; the estimated electronic coupling, H_{ab}, is similar to or even higher than the internal barrier. Moreover, this ET system reveals the importance of nuclear tunneling. For example, an intramolecular ET rate with a time scale shorter than 10^{-10} s was reported for I_2BFC^+ in the crystalline state, even at 4 K.[15c,39a] Considering these points, we regard the effective reaction barrier along the internal coordinate, q, to be much smaller than the solvent reorganization energy in the present ET system. The ET rate is then approximated by[53,54]

$$k_{et} \approx \nu_n \exp(-\lambda_{os}/4RT) \tag{7a}$$

$$\nu_n \approx (2\tau_s)^{-1}(\lambda_{os}/4\pi RT)^{1/2} \tag{7b}$$

The ET rate is thus dominated by the process along the solvent coordinate, and as can be seen in eq 7, the solvation relaxation time, τ_s, directly controls the ET rate. If a solvent is regarded as a dielectric continuum, then τ_s is equal to the dielectric longitudinal relaxation time, τ_L, of the solvent. The k_{et} values in acetone at various temperatures, calculated on the assumption that $\tau_s = \tau_L$, are shown in Figure 4. The calculated values were lower and the temperature slopes somewhat steeper than those observed. The common underestimation in the calculations for the subject mixed-valence monocations can probably be ascribed to the effective solvation times, τ_s, being smaller than τ_L.

The solvation relaxation time, τ_s, in eq 7 corresponds to the relaxation time of the solvation free energy for the new electronic charge configuration generated by the ET reaction. Such solvation relaxation times are individually observed by the time-dependent Stokes shifts in the luminescence of dyes after photoexcitation in a polar medium. However, most of the averaged relaxation time observed for probe dyes with relatively large dipole changes on photoexcitation indicates a rather longer relaxation time than τ_L.[12] Theories based on a dielectric continuum model also predict a longer relaxation time than τ_L.[12b,55] On the other hand, the relaxation time exhibits a probe dependence, as shown in recent studies of a reference interaction site model (RISM) theory.[13b] The dipole changes on the ET, $\Delta\mu$, (estimated to be ~3.5 D for the ET reactions of BFC^+)[46] is considerably smaller than those for the photoexcitations of most of the probe dyes: e.g., $\Delta\mu \approx 7.5-9.5$ D for coumarin 153 (C153).[56] Furthermore, the two iron atoms, which take the central role in the charge migrations, are surrounded by the cyclopentadienyl rings. In contrast, in many of the probe dyes, oxygen and/or nitrogen atoms with relatively high charge densities, particularly in the electronically excited state(s), are exposed to the solvent. The restricted space available for charge movement, roughly equal to the dimension of solvent molecules, or the weaker perturbation to the solvent may elicit the shorter effective solvation times.

The effect of the solvent dynamics on the solvent dependence of the ET rates is directly reflected in the pre-exponential factors, ν_n, as shown in eq 7. To evaluate the contribution of the dielectric continuum mode of the solvent to the dynamics along the solvent coordinate of the ET reaction, we have plotted the logarithms of the observed pre-exponential factors, $\nu_{n(obs)} =$

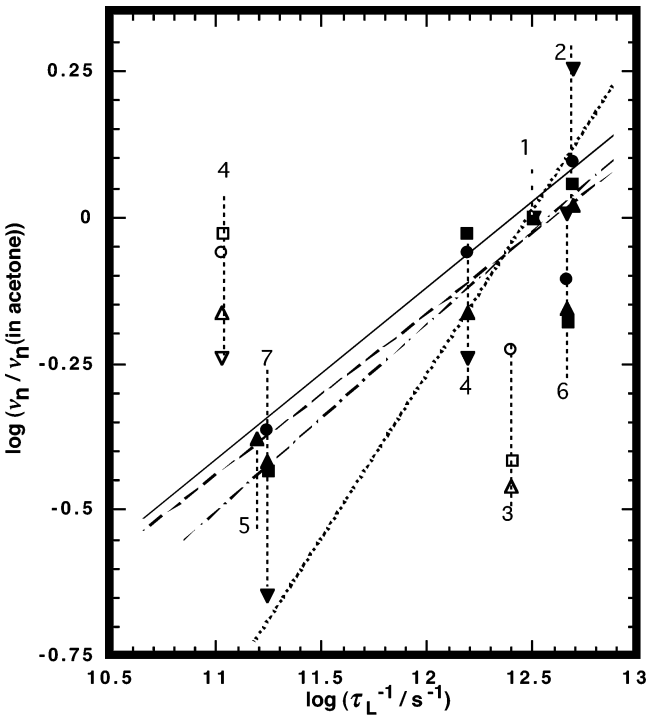

Figure 6. Plots of observed pre-exponential factors, ν_n, relative to those in acetone against longitudinal dielectric relaxation times, τ_L: BFC^+ (closed circle), Et_2BFC^+ (closed triangle), I_2BFC^+ (closed square), and DFA^+ (closed inverted triangle) at 298 K, except for those in dichloromethane and methanol. The data in dichloromethane are indicated by open symbols. The open and closed symbols for methanol are, respectively, plots against the relaxation times for the main relaxation, τ_1, and that for the fastest relaxation component, τ_3, assuming multiple (three) relaxations. The numbers in the figure indicate the following: 1, acetone; 2, acetonitrile; 3, dichloromethane; 4, methanol; 5, ethylene glycol; 6, nitromethane; 7, nitrobenzene. Solid, dashed, dot−dashed, and dotted lines indicate the least-squares fitting results, respectively, for BFC^+, Et_2BFC^+, I_2BFC^+, and DFA^+, excluding the data in dichloromethane. For methanol, the plots against τ_3 are used for the fittings instead of those against τ_1.

$k_{et(obs)}/\exp(-\lambda_{os}/4RT)$, relative to those in acetone against τ_L^{-1} in Figure 6.[57] In most of the solvents, a roughly linear relation can be seen in the logarithm plot for each monocation. However, the slopes, β, given by a least-squares fitting for the plots in Figure 6 are less than unity for all the monocations; thus, the coupling with the solvent as a dielectric continuum is insufficient. The obtained β values for the acetylene-bridged biferrocene monocation, DFA^+, with the longer ET distance, are significantly larger than those for BFC^+, I_2BFC^+, and Et_2BFC^+; i.e., a charge migration with a larger space increases the coupling with a solvent dielectric medium.

Such behavior of the solvent dynamical effect is phenomenologically quite similar to that seen in molecular rotation. The experimental results giving β values for the logarithm plots of the observed rotational relaxation times of polar molecules or ions against those calculated on the basis of dielectric friction models suggest that the contribution of the dielectric friction of the solvent becomes insufficient with decreasing the molecular (ionic) sizes or the magnitudes of the multipoles.[58]

In dichloromethane, the ν_n value for each mixed-valence monocation is significantly low compared with those in the other solvents, as shown by the open symbols in Figure 6. Due to the low dielectric constant of the solvent, low energy shifts of the IT band maxima of BFC^+ and DFA^+ in dichloromethane, ascribed to ion pairing, were observed even at concentrations much less than 0.5 mM of the monocations.[15e,59] The electric field relaxation caused by the configurational fluctuation and the dissociation of the ion pair is a significant contributor to the τ_s value in eq 8, since the ion pair formation affects the outer sphere reorganization energy. The field relaxation by the counteranion, with a much slower time scale than that of the dielectric relaxation of the solvent, thus brings about the low $\nu_{n(obs)}$ values in dichloromethane. Such a decrease in ET rates or pre-exponential factors by slow counterion dynamics is also found in the intramolecular ETs of organic radicals.[60]

4.3. ET Rates in Methanol. A characteristic behavior in methanol found in the plots in Figure 6 (symbols numbered 4) is worthy of comment. The dielectric relaxation of methanol shows a non-Debye multiple relaxation behavior, and the main relaxation is abnormally long, 51 ps, compared with the other solvents used in the present study.[61] The observed ν_n values in methanol were, however, comparable to those in the other solvents. On the other hand, the plots of ν_n against the relaxation times of the minor components with shorter relaxation times, which are assigned to such local motions of methanol as the OH group reorientation, (indicated by the closed symbols numbered 4 in Figure 6), approach the trend of the other solvents. This result indicates that the rapid and local solvent dynamics exerts more control over the ET rate than the slower main relaxation component, which is assigned as the relaxation of an alcohol chain-like cluster structure. The solvent relaxation, with a similar scale in time and space to the charge migration in the ET process, effectively generates the friction for the reaction dynamics along the solvent coordinate. In contrast, the relaxation of a mesoscale alcohol chain-like structure does not participate in the ET rates. A similar behavior in alcohols is also found for the rotation of small molecules (ions); that is, the contribution of the faster dielectric relaxation to the rotational friction is relatively important compared to that of the slower main relaxation.[58] On the other hand, the average solvation relaxation time derived from measurements of the time-dependent Stokes shift of C153 in alcohols is about 1 order of magnitude longer than that in acetone.[62]

A similar characteristic behavior in methanol is found in the Pekar plots of the reorganization energies in Figure 3; the use of the dielectric constants for the fastest (minor) dielectric relaxation components (closed symbols numbered 4) enables the plots in alcohols to approach the trend of the plots of the other solvents. This result also indicates that, as conjectured from the observed ET rates in alcohols, the slow main relaxation modes of the alcohols scarcely respond to the solvent reorganization due to the electron hopping between two iron ions.

5. Conclusion

The intramolecular ET rates of the mixed-valence biferrocene monocation in various solvents were determined by the proton spin−lattice relaxation measurements, evaluating the contribution to the rates of local field fluctuation caused by electron hopping between the two iron atoms. The observed rates were decreased by the insertion of an acetylene bridge between the two ferrocene units, but the effect on the rates of substitution on the cyclopentadienyl rings was minor. The rates for each monocation in different solvents did not correlate with the reorganization energies, but were noticeably retarded in viscous solvents.

The solvent dynamic contribution was analyzed on the basis of the Sumi−Marcus−Nadler model. The subject system is considered to be controlled mainly by the dynamics along the solvent coordinate. The comparison of the observed rates or the pre-exponential factors, ν_n, to those calculated regarding the

solvent as a dielectric continuum indicated that the solvent dielectric friction was partly responsible for the dynamics along the solvent coordinate, and that the extent of its contribution for DFA^+ was larger than those for BFC^+, I_2BFC^+, and Et_2-BFC^+. These results suggest that the extent of the dielectric friction effect depended on the ET distance or the dipole change between the reactant and product.

Acknowledgment. This work was partially supported by Grants-in-Aid for Scientific Research, no. 12640489 from the Ministry of Education, Science and Culture. The authors express their acknowledgment to Ms. A. Ushiro for the synthesis of diferrocenylacetylene.

6. Appendix

This section describes a procedure to determine the hyperfine coupling constant, A. Assuming axial symmetry for the g tensor and the isotropic hyperfine interaction, the NMR shift caused by the interaction with the electron spin, $(\Delta\nu/\nu_0)_{para}$, is represented by[31]

$$(\Delta\nu/\nu_0)_{para} = (\Delta\nu/\nu_0)_{hyp} + (\Delta\nu/\nu_0)_{dip} \quad \text{(A1a)}$$

$$(\Delta\nu/\nu_0)_{dip} = (^1/_{45})\beta^2 S(S+1)(k_B T)^{-1} r_{IS}^{-3} (1 - 3\cos^2\theta)(g_{||} - g_{\perp}) \times (3g_{||} + 4g_{\perp}) \quad \text{(A1b)}$$

$$(\Delta\nu/\nu_0)_{hyp} = -(^1/_{45})\beta S(S+1)(\hbar\gamma_H k_B T)^{-1}(3g_{||} + 2g_{\perp})A \quad \text{(A1c)}$$

where $(\Delta\nu/\nu_0)_{hyp}$ and $(\Delta\nu/\nu_0)_{dip}$ indicate the shifts caused by the hyperfine and dipolar interactions, respectively. The values of $(\Delta\nu/\nu_0)_{para}$ for the mixed-valence monocations were determined from the shift difference between the monocations and the respective neutral biferrocenes. In the present systems, the doubled values of the observed shift difference were used for $(\Delta\nu/\nu_0)_{para}$ because the NMR spectra of the fulvalene protons were averaged over those in the ferrocene and the ferrocenium site (see Figure 1). Thus, experimentally obtained $(\Delta\nu/\nu_0)_{para}$ values were compared with the $(\Delta\nu/\nu_0)_{dip}$ values calculated according to eq A1b, with the g values determined by the ESR and the crystal structural data. The results shown in Table 1 indicate that the contribution of the dipolar interaction to the $(\Delta\nu/\nu_0)_{para}$ term is negligible. Thus, the paramagnetic shift is mainly attributed to the hyperfine term, $(\Delta\nu/\nu_0)_{hyp}$. The hyperfine coupling constant can then be obtained from the observed shifts and the g values according to eq A1c.

Supporting Information Available: Table of observed proton spin−lattice relaxation times and intramolecular electron-transfer rate constants of BFC^+, Et_2BFC^+, I_2BFC^+, and DFA^+ in various solvents at various temperatures. This material is available free of charge via the Internet at http://pubs.acs.org.

References and Notes

(1) See, for example, (a) *Dynamics and Mechanisms of Photoinduced Electron Transfer and Related Phenomena*; Mataga, M., Okada, T., Masuhara, H., Eds.; Elsevier: Amsterdam, 1992. (b) A special issue on "Electron Transfer". *Chem. Rev.* **1992**, C92. (c) Marcus, R. A.; Sutin, N. *Biochim. Biophys. Acta* **1985**, *81*, 1265. (d) Newton, M. D.; Sutin, N. *Annu. Rev. Phys. Chem.* **1984**, *35*, 437.

(2) Marcus, R. A. *J. Chem. Phys.* **1956**, *24*, 988,

(3) Marcus, R. A. *J. Chem Phys.* **1965**, *43*, 679.

(4) Barbara, P. F.; Jarzeba, W. *Adv. Photochem.* **1990**, *15*, 1.

(5) Kosower, E. M.; Huppert, D. *Annu. Rev. Phys. Chem.* **1986**, *37*, 127.

(6) Maroncelli, M.; MacInnis, J.; Fleming, G. R. *Science* **1989**, *243*, 1670.

(7) Weaver, M. J.; McManis, G. E. *Acc. Chem. Res.* **1990**, *23*, 294.

(8) Barbara, P. F.; Walker, G. C.; Smith, T. P. *Science* **1992**, *256*, 975.

(9) Heitele, H. *Angew. Chem., Int. Ed.* **1993**, *32*, 359.

(10) (a) Sumi, H.; Marcus, R. A. *J. Chem. Phys.* **1986**, *84*, 4272; (b) **1986**, *84*, 4894.

(11) Nadler, W.; Marcus, R. A. *J. Chem. Phys.* **1987**, *86*, 3906.

(12) (a) Maroncelli, M. *J. Mol. Liq.* **1993**, *57*, 1. (b) Horng, M. L.; Gardeccki, J. A.; Papazyan, A.; Maroncelli, M. *J. Phys. Chem.* **1995**, *99*, 17311, and references therein.

(13) (a) Su, S.-G.; Simon, J. D. *J. Phys. Chem.* **1989**, *93*, 753. (b) Nishiyama, K.; Hirata, F.; Okada, T. *J. Chem. Phys.* **2003**, *118*, 2279. (c) Biswas, R.; Bagchi, B. *J. Phys. Chem.* **1996**, *100*, 1238.

(14) (a) Heitele, H.; Michel-Beyerle, M. E.; Finckh, P. *Chem. Phys. Lett.* **1987**, *134*, 273. (b) Tominaga, K.; Kliner, D. A. V.; Johnson, A. E.; Levinger, N. E.; Barbara, P. F. *J. Chem. Phys.* **1993**, *98*, 1228.

(15) (a) Kaufman, F.; Cowan, D. O. *J. Am. Chem. Soc.* **1970**, *92*, 6198. (b) Cowan, D. O.; Condela, G. A.; Kaufman, F. *J. Am. Chem. Soc.* **1971**, *93*, 3889. (c) Morrison, W. H.; Hendrickson, D. N. *Inorg. Chem.* **1975**, *14*, 2331. (d) Dong, T. Y.; Kambara, T.; Hendrickson, D. N. *J. Am. Chem. Soc.* **1986**, *108*, 4423. (e) Lowey, M. D.; Hammack, W. S.; Drickamer, H. G.; Hendrickson, D. N. *J. Am. Chem. Soc.* **1987**, *109*, 8019.

(16) (a) Masuda, A.; Masuda, Y.; Fukuda, Y. *J. Phys. Chem. A* **1997**, *101*, 2245. (b) Masuda, A.; Masuda, Y. *J. Mol. Liq.* **1996**, *65*, 397.

(17) Bolton, J. R.; Mataga, N.; McLendon, G. *Electron Transfer in Inorganic, Organic, and Biological Systems*; American Chemical Society: Washington, DC, 1991.

(18) Jortner, J.; Bixon, M. *Protein Structure; Molecular and Electronic Reactivity*; Austin, R., Buhks, E., Chance, B., Voult, D., Dutton, P. L., Fauenfelder, H., Gol'danski, V. I., Ed.; Saringer: New York, 1987; p 277.

(19) (a) Robin, M. B.; Day, P. *Adv. Inorg. Chem. Radiochem.* **1967**, *10*, 247. (b) Creutz, C. *Prog. Inorg. Chem.* **1983**, *30*, 1.

(20) (a) Jordan, K. D.; Paddon-Row, M. N. *Chem. Rev.* **1992**, *92*, 395. (b) Nelsen, S. F. *Adv. Electron Transfer Chem.* **1993**, *3*, 167.

(21) (a) Ito, T.; Hamaguchi, T.; Nagino, H.; Yamaguchi, T.; Washington, J.; Kubiak, C. P. *Science* **1997**, *277*, 660. (b) Ito, T.; Hamaguchi, T.; Nagino, H.; Yamaguchi, T.; Kido, H.; Zavarine, I. S.; Richmond, T.; Eashington, J.; Kubiak, C. P. *J. Am. Chem. Soc.* **1999**, *121*, 4625.

(22) (a) Rausch, M. D. *J. Org. Chem.* **1961**, *26*, 1802. (b) Fish, R. W.; Rosenblum, M. *J. Org. Chem.* **1965**, *30*, 1253. (c) Shechter, H.; Helling, J. F. *J. Org. Chem.* **1961**, *26*, 1034.

(23) Kovar, R. F.; Rausch, M. D.; Rosenberg, H. *Organomet. Chem. Synth.* **1970**, *1*, 173.

(24) Iijima.; S. Saida, R.; Motoyama, I.; Sano, H. *Bull. Chem. Soc. Jpn.* **1981**, *54*, 1375.

(25) Rosenblum, M.; Brawn, N.; Papenmeier, J.; Applebaum, M. *J. Organomet. Chem.* **1966**, *6*, 173.

(26) Dong, T.-Y.; Kambara, T.; Hendrickson, D. N. *J. Am. Chem. Soc.* **1986**, *108*, 4423.

(27) The classification of protons in the fulvalene or the cp rings was carried out by H−H COSY measurements. The protons with relatively longer T_1 values were assigned to the cp rings, in the consideration of the internal rotation of the cp rings around the pseudo C5 axes (see ref 28). The protons with longer T_1 values within the fulvalene or the cp rings were, respectively, assigned to fv1 and cp1 (see Figure 1), because absent appreciable rotational anisotropy, the proton spin−lattice relaxation times were taken as proportional to the numbers of the neighboring proton(s). The proton signals with the T_1 values, e.g., 11.2 s, 14.1 s, 25.1 s, and 16.7 s, for I_2BFC in acetone were thus assigned, respectively, to fv2, fv1, cp1, and cp2.

(28) Longer T_1 values for the cyclopentadienyl protons than for the fulvalene protons were observed in all the mixed-valence monocations in the present study, indicating that the correlation times for the cyclopentadienyl protons, τ_c, in eqs 3a and 4a, are smaller due to the participation of the internal rotation of the cyclopentadienyl rings.

(29) The T_1 values for the mixed-valence biferrocene, BFC^+, in the present study (measured at 9.4 T) are about 20−30% shorter than those in our previous paper (ref 16). This difference may be attributed to a higher extent of overlap of the proton signals with those of the cp rings with longer T_1 in the previous study, because the measurements in that study were carried out at lower magnetic field (6.4 T).

(30) The paramagnetic contribution of the unpaired electron to the relaxation rates of the protons is negligibly small for those in the fc unit (Fe(II), $S = 0$) compared with those in the ferrocenium unit (Fe(III), $S = {}^1/_2$), because the proton relaxation rates, caused by the dipolar interaction with the electron spin or by the hyperfine interaction, depend, respectively, on the −6th powers of the distance between the proton and the electron spin or on the magnitude of the hyperfine parameter.

(31) Swift, T. J.; La Mar, G. N.*NMR of Paramagnetic Molecules*; La-Mar, G. N., Horrocks, W. D., Jr., Holm, R. H., Eds.; Academic Press: New York, 1973; Chapters 1 and 2.

(32) Banci, L.; Bertini, I.; Luchinat, C. *Nuclear and Electron Relaxation*; VCH Publishers: New York, 1991; Chapter 5.

(33) Farrar, T. C.; Becker, E. D. *Pulse and Fourier Transform NMR*; Academic Press: New York, 1971; Chapter 4.

(34) These relations are also satisfied at the other temperatures and in the other solvents used in ref 16. The experimental conditions in ref 16 almost cover those in the present study.

(35) (a) Steele, W. A. *Adv. Chem. Phys*. **1986**, *34*, 1. (b) Masuda, Y.; Yamatera, H. *Structure and Dynamics of Solution*; Ohtaki, H., Yamatera, H., Eds.; Elsevier: Amsterdam, 1992; Chapter 4.

(36) The T_{2e} values of the mixed-valence biferrocene and the derivatives were estimated by comparing the ESR line widths with that for fc^+. (See refs 15b, 16, and 37.)

(37) Prins, R.; Reinder, F. J. *J. Am. Chem. Soc*. **1969**, *91*, 4929.

(38) No appreciable difference was found between the observed *g* values in the frozen solutions and those in powder samples. (See ref 39.)

(39) (a) Dong, T.-Y.; Hendrickson, D. N.; Pierpont, C. G.; Moore, M. E. *J. Am. Chem. Soc*. **1986**, *108*, 963. (b) Nakashima, S.; Masuda, Y.; Motoyama, I.; Sano, H. *Bull. Chem. Soc. Jpn*. **1987**, *60*, 1673.

(40) Dong, T.-Y.; Hendrickson, D. N.; Iwai, K.; Cohn, M. J.; Geib. S. J.; Rheingold, A. L.; Sano, H.; Nakashima, S. *J. Am. Chem. Soc*. **1985**, *107*, 7996.

(41) Common r_{IS} and θ values ($r_{IS} = 2.85$ Å, $\theta = 53.9°$) were used for the all of the mixed-valence monocations in the present study because a variation in the distance and the angle in each mixed-valence monocation caused by the crystal packing or the counteranion is similar to or even exceeds that by difference in the substituents on the cp rings. (See refs 15d, 39, 40.)

(42) (a) Sutin, N. *Adv. Chem. Ser*. **1991**, *228*. 25. (b) Brunschwig, B. S.; Creutz, C.; Sutin, N. *Chem. Soc. Rev*. **2002**, *31*, 168. (c) Brunschwig, B. S.; Sutin, N. *Electron Transfer in Chemistry*; Balzani, I., Ed.; Wiley-VCH: New York, 2001; Vol. 2, p 583.

(43) (a) Creutz, C.; Newton, M. D.; Sutin, N. *J. Photochem. Photobiol*. **1994**, *A82*, 47. (b)Hush, N. S. *Prog. Inorg. Chem.* **1967**, *8*, 391.

(44) An effective value for the dipole moment change for BFC^+ (3.5 eÅ), which reproduced the outer-sphere reorganization energy estimated from an ellipsoidal cavity model (e.g., Brunschwig, B. S.; Ehrenson, S.; Sutin, N. *J. Phys. Chem.* **1986**, *90*, 3657) was used instead of the value (5.1 eÅ) based on the distance between the two iron ions (see ref 45). This value was also used for $Et2BFC^+$ and $I2BFC^+$. Similarly, a value of 5.4 e Å was assumed for DFA^+.

(45) (a) Iijima, S.; Motoyama, I.; Sano, H. *Bull. Chem. Soc. Jpn*. **1980**, *53*, 3180. (b) Dong, T. Y.; Schei, C. C.; Hsu, T. L. Lee, S. L.; Li, S. J. *Inorg. Chem*. **1991**, *30*, 2457. (c) Powers, M. J.; Meyer, T. J. *J. Am. Chem. Soc.* **1978**, *100*, 4393.

(46) Williams, R. D.; Vladimir, I. P.; Lu, H. P.; Hupp, J. T. *J. Phys. Chem. A* **1997**, *101*, 8070.

(47) In ref 45, a contribution of energy splittings by spin−orbit couplings and a dynamic Jahn−Teller effect to the band maxia, ν_{max}, of the IT absorption of BFC^+ is estimated to be about 300 cm^{-1}. The sum of the contribution and the vibrational reorganization energy, ∼37 kJ mol^{-1}, corresponds to the 0-intercept in the Pekar plot because the solvent dependences of the values are negligible. The estimated value is similar to those experimentally obtained.

(48) McManis, G. E.; Gochev, A.; Nielson, R. M.; Weaver, M. J. *J. Phys. Chem.* **1989**, *93*, 7733.

(49) For the fitting, the data in dichloromethane are excluded. For methanol, the plots against the Pekar factor corresponding to the fastest relaxation assuming multiple (three) dielectric relaxations of the solvent, $\epsilon_{op}^{-1} - \epsilon_3$, are used for the fitting insted of those against $\epsilon_{op}^{-1} - \epsilon_s^{-1}$ (see section 4.2).

(50) (a) Ruff, I.; Korösi-Ódor, I. *Inorg. Chem.* **1970**, *9*, 186. (b) Ruff, I.; Friedrich, V. J.; Demeter, K.; Csillag, K.; *J. Phys. Chem*. **1971**, *75*, 3303.

(51) Yang, E. S.; Chan, M.−S.; Wahl, C. *J. Phys. Chem*. **1980**, *84*, 3094.

(52) Nielson, R. M.; McManis, G. E., Golovin, M. N.; Weaver, J. M. *J. Phys. Chem*. **1988**, *92*, 3441.

(53) Zhu, J.; Rasaiah, J. C. *J. Phys. Chem*. **1991**, *95*, 3325.

(54) This representation is equivalent to that for the solvent-controlled ET rate at the strong adiabatic limit.

(55) Bagchi, B.; Chandra, A. *Adv. Chem. Phys*. **1991**, *80*, 1

(56) (a) Moylan, C. R.; *J. Phys. Chem*. **1994**, *98*, 13513. (b) Reynolds, L.; Gardecki, J. A.; Frankland, S. J. V.; Horng, M. L.; Maroncelli, M. *J. Phys. Chem*. **1996**, *100*, 10337.

(57) The plots of $k_{et(obs)}/\exp(-\lambda_{os}/4RT)$, i.e., ν_n (obs) versus ν_n given by eq 7, show a qualitatively similar result.

(58) Hosoi, H.; Masuda, Y. *J. Phys. Chem. B* **1998**, *102*, 2995. Masuda, Y. *J. Phys. Chem. A* **2001**, *105*, 2989.

(59) Blackbourn, R. L.; Hupp, J. T. *J. Phys. Chem*. **1990**, *94*, 1788.

(60) Hosoi, H.; Masuda, Y. *J. Mol. Liq.* **2005**, *119*, 89.

(61) (a) Barthel, J.; Bachhuber, K.; Buchner, R.; Hetzenauer, H. *Chem. Phys. Lett*. **1990**, *165*, 369. (b) Turq, P.; Bathel, J.; Chemla, M. *Transport, Trlaxation, and Kinetic Process in Electrolyte Solutions*; Springer-Verlag: Berlin, 1992; Lecture Notes in Chemistry, Vol 57, Chapter VII.

(62) Kumar, P. V.; Maroncelli, M. *J. Chem. Phys.* **1995**, *103* (22), 3038.